BROADBAND DIELECTRIC SPECTROSCOPY OF DIELECTRIC-CONDUCTOR COMPOSITES: CHARACTERIZATION OF PHYSICAL PROPERTIES AND APPLICATION POTENTIAL

Viktor Bovtun, Jan Petzelt, Dmitry Nuzhnyy, Martin Kempa, Maxim Savinov

Institute of Physics, Department of Dielectrics, Czech Academy of Sciences,
Na Slovance 2, 18221 Prague, Czech Republic
Email: bovtun@fzu.cz, Web Page: http://www.fzu.cz

Keywords: nanocomposites, dielectric spectra, microwave absorption, shielding efficiency

Abstract
Composites of dielectric matrix filled with conductive filler are electrically inhomogeneous materials with frequency dependent dielectric properties and conductivity. We demonstrate here that broadband dielectric spectroscopy (1 mHz – 1 THz) can reveal essential information on the composition-structure-properties relation, conductivity mechanisms, percolation phenomena, etc. of dielectric-conductor composites. Dielectric spectra can be also used for analysis of the shielding efficiency and microwave absorption of composites in the high-frequency, microwave and THz ranges that allows estimation of their potential for the electromagnetic applications. This approach was applied to three types of composites: polymer-matrix composites of poly(ethylene terephthalate) and multiwalled carbon nanotubes; ceramic-matrix composites of alumina and carbon nanofibers; variously conducting polyaniline pellets composed of the more-conducting crystalline nanoregions and less-conducting amorphous ones.

1. Introduction

Composites of dielectric matrix filled with conductive filler are electrically inhomogeneous materials. Electrically inhomogeneous structure of the dielectric-conductor composites (DCC) is responsible for the dielectric and AC conductivity dispersion in a very broad frequency range, including microwave (MW) frequencies [1-4]. Present facilities in the Department of Dielectrics, Institute of Physics, Czech Academy of Sciences, enable us to study the complex dielectric/conductivity response of various dielectric, semiconducting and poor-metallic conducting materials in the frequency range of 10^{-5}-10^{13} Hz using standard low frequency (LF) impedance spectroscopy below ~1 MHz, coaxial, waveguide and strip-line techniques in the high-frequency (HF) and MW range 1 MHz - 50 GHz, quasi-optic time-domain terahertz (THz) spectroscopy usually in the range of 0.1 – 3 THz. Application of this broadband dielectric spectroscopy (BDS) allows study of all possible polarization, loss and conductivity mechanisms in the electrically inhomogeneous materials below phonon frequencies.

We demonstrate here that BDS can reveal essential information on the composition-structure-properties relation, conductivity mechanisms, percolation phenomena, etc. of DCC. Dielectric spectra can be also used for analysis of the shielding efficiency (SE) and microwave absorption (MA) of composites in the high-frequency, microwave and THz ranges that allows estimation of their potential for the electromagnetic applications. We analyze and discuss dielectric spectra (i.e., frequency dependences of complex dielectric permittivity $\varepsilon^* = \varepsilon' - i\varepsilon''$ consisting of the dielectric permittivity ε' and loss ε") and conductivity (σ') spectra of the following composites:

Excerpt from ISBN 978-3-00-053387-7

a) Polymer-matrix composites of poly(ethylene terephthalate) and multiwalled carbon nanotubes (PET-xCNT, x = 0–3 vol.% is the fraction of CNT) [3];
b) Ceramic-matrix composites of alumina and carbon nanofibers (alumina-xCNF, x = 0–9 vol.% is the fraction of CNF) [4];
c) Variously conducting polyaniline pellets (conducting c-PANI, semi-conducting sc-PANI and non-conducting nc-PANI) composed of the more-conducting crystalline nanoregions (~10 nm) and less-conducting amorphous ones [2].

2. Dielectric Spectra and Physical Properties of DCC

2.1. PET-xCNT Composites

Dielectric dispersion in a broad frequency range was observed for all PET-xCNT compositions (Fig. 1) and attributed to the charge transfer mechanisms in CNT clusters [2,3]. It was shown that in addition to the DC conductivity of percolated CNT clusters, the AC conductivity of CNT in the finite clusters contributes to the dielectric spectra. Broadband conductivity spectra (Fig. 2a) show quite well the universal conductivity behaviour characteristic for disordered weak conductors [1] with a low-frequency plateau corresponding to DC conductivity. This plateau appears above the electrical percolation threshold, increases and broadens with increasing CNT concentration. In the higher frequency range, where AC conductivity increases with frequency, obeying roughly a power law up to the THz range, conductivity increases with concentration. The AC conductivity of PET-xCNT composites achieves high values σ' ~4 S/cm at 1 THz.

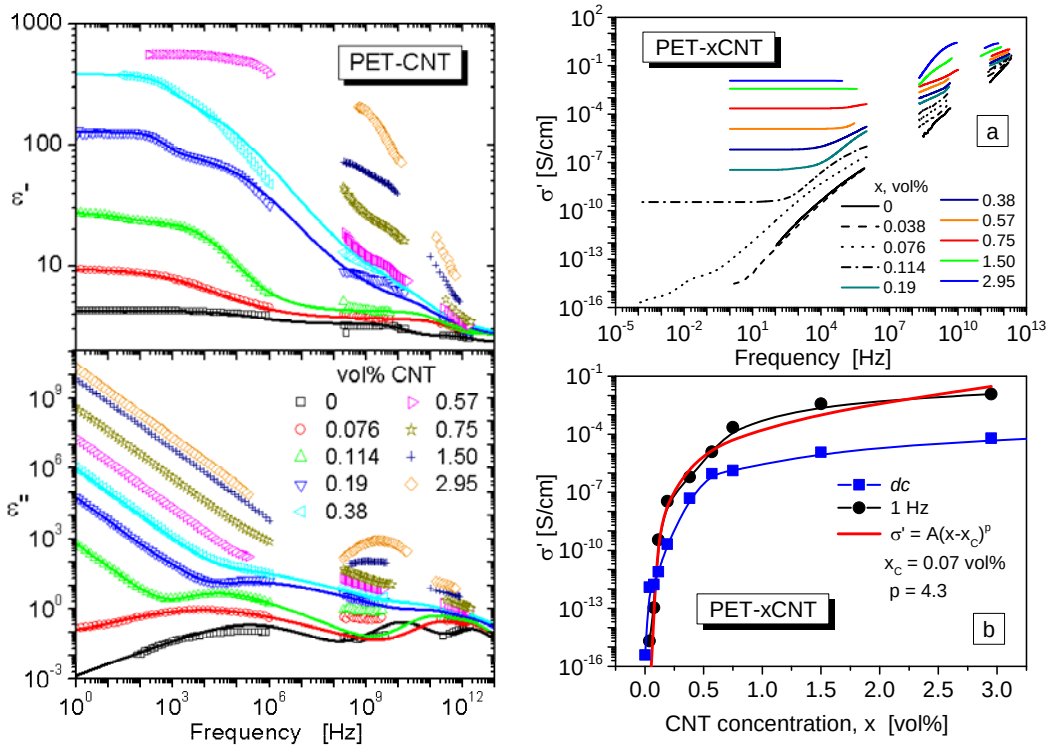

Figure 1. Frequency dependences of dielectric permittivity (ε') and loss (ε'') of PET-xCNT composites. Symbols denote experimental points, lines are phenomenological fits.
Figure 2. Frequency (a) and concentration (b) dependences of conductivity (σ') of PET-xCNT composites. Symbols in (b) denote experimental points, red line is a power law fit with percolation threshold x_C = 0.07 vol.%.

Excerpt from ISBN 978-3-00-053387-7

Deviations from simple universal conductivity behavior were observed. Percolation threshold of $x_C \approx$ 0.07 vol.% CNTs in PET-xCNT were revealed from the low-frequency conductivity plateau corresponding to the DC conductivity in percolated CNT clusters (Fig. 2b). This value corresponds well to the threshold concentration estimated by DC conductivity measurements [3]. On the other hand, LF permittivity continuously increased with CNT concentration, indicating a more complex AC conductivity behavior of neat CNTs. Temperature dependence of the LF conductivity [3] shows semiconductor behavior down to 5 K and is compatible with the fluctuation-induced tunneling behavior [5] through a thin (~1 nm) polymer contact interface between all adjacent CNTs within the percolated clusters, with a low extrapolated zero-temperature (tunneling) DC conductivity and low activation energy of ~3 meV, independent of CNT concentration.

Accounting for multiple conductivity or polarization mechanisms, dielectric spectra of several PET-xCNT composites were modeled by a set of phenomenological Cole-Cole relaxations, one overdamped THz oscillator and a Drude term describing LF conductivity plateau above the percolation threshold [2,3]. The resulting fitted spectra for selected compositions are shown in Fig. 1 together with the experimental ones. The low percolation threshold and easy modification of MW dielectric properties by the change of CNT concentration make PET-xCNT composites attractive for electromagnetic (EM) applications.

2.2. Alumina-xCNF Composites

Dielectric and conductivity spectra of alumina-xCNF composites [4] are shown in Fig. 3. Similar to the PET-xCNT composites, dielectric dispersion and the universal conductivity behavior with LF plateau corresponding to DC conductivity in percolated CNF clusters and further AC conductivity increase with frequency toward the THz range corresponding to the localized charge transport in the non-percolated CNF clusters are observed. Percolation threshold of ~2 vol.% of CNF was revealed from the LF conductivity plateau.

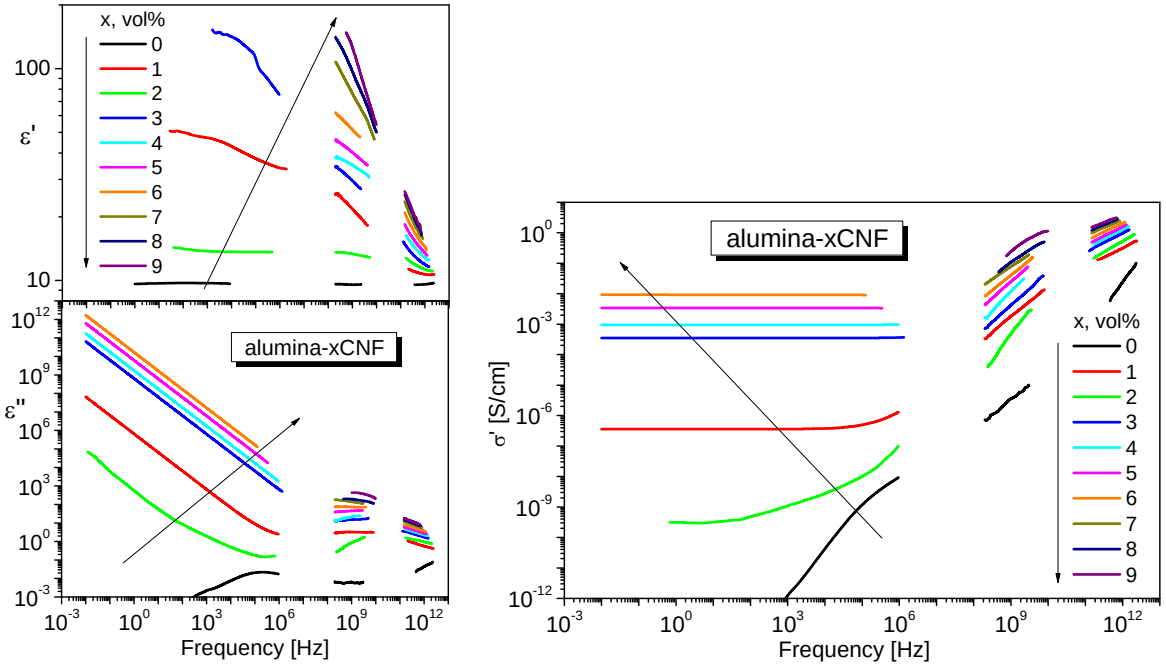

Figure 3. Frequency dependences of dielectric permittivity (ε'), loss (ε'') and AC conductivity (σ') of alumina-xCNF composites.

Excerpt from ISBN 978-3-00-053387-7

Differently from the PET-xCNT composites, the LF and HF dielectric and conductivity properties depend not only on the CNF concentration, but also on the alumina grain size and topology of the composites. In particular, the pinning effect of small carbon particles on alumina grains modifies the spatial distribution of the conducting phase. This effect has a significant influence on the electromagnetic properties of the composites: actually the percolation threshold is reached twice (Fig. 4a), below 1 and close to 2 vol.% of CNF as the result of the change of local CNF concentration [4]. This unusual phenomenon is also caused by the strong influence of the CNF content on the alumina grain size below 2 vol.% of CNF (Fig. 4b). The THz properties are mainly defined by the CNF concentration and are less sensitive to the composite morphology. Therefore they monotonically change with increasing CNF concentration, while the LF and HF ones show an anomaly near 2 vol.% (Fig.3 and Fig.4).

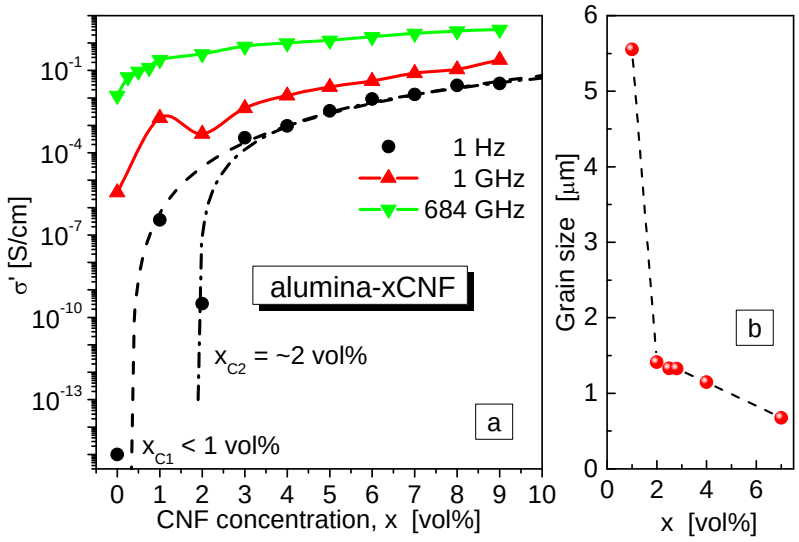

Figure 4. Concentration dependences of AC conductivity at different frequencies (a) and alumina grain size (b) of alumina-xCNF composites. Dash lines in (a) are power law fits with percolation thresholds x_{C1} < 1 vol.% and x_{C2} = ~2 vol.%.

2.3. Variously Conducting PANI

PANI has nano-inhomogeneous conductivity, mainly due to its semi-crystalline structure, where the crystalline nanoregions (~10 nm) are usually more conducting than the amorphous ones. Therefore the AC conductivity of PANI can be modeled as that of composites. Dielectric and AC conductivity spectra of the variously conducting PANI pellets show a standard behavior of nano-inhomogeneous or composite conductors with the low-frequency plateau of conductivity and dielectric dispersion in a broad frequency range [2]. Their DC conductivity corresponding to the low-frequency plateau level varies from ~10^{-12} S/cm for nc-PANI to ~10^{-5} S/cm for sc-PANI and ~1 S/cm for c-PANI. Dielectric spectra of PANI were modeled similar to that of the PET-CNT composites by a set of phenomenological Cole-Cole relaxations, one overdamped THz oscillator and a Drude term describing the low-frequency conductivity [2].

DC conductivity of the semiconducting PANI is thermally activated (E_a = 0.305 eV) at T>180 K; at low temperatures some small background T = 0 tunneling DC conductivity of 10^{-15} S/cm remains [2]. DC conductivity of the conducting PANI is thermally activated below ~100 K and corresponds equally well to the variable-range hopping model and the fluctuation induced tunneling model, both models differ only below ~10K [2].

Excerpt from ISBN 978-3-00-053387-7

3. Absorbing and Shielding Properties of DCC

Dielectric-conductor composites belong to effective absorbing and shielding materials which are widely used in electronics and telecommunications, military and civilian MW techniques [6-8]. Electrically inhomogeneous structure of DCC is responsible for the dielectric dispersion in a very broad frequency range, including MW frequencies [1-4] and consequently results in a high level of their electromagnetic (EM) field absorption at HF, MW and even THz frequencies.

Microwave absorbing and shielding properties of materials are usually estimated in two ways [6,7,9,10]. The first one is based on direct experimental measurements of reflection and transmission coefficients of the material layer or multilayer structure in free space or transmission line (waveguide). But for the free space microwave measurements, big samples are required. The waveguide measurements can be performed with smaller samples, but usually in the relatively narrow frequency range. These problems limit practical application of the direct experimental measurements. The second way is simulations, model calculations based on the measured (usually, at a single frequency) or a priori taken values of dielectric permittivity and losses (or conductivity). Consequently, dielectric dispersion is not accounted. But DCC are characterized by the strong frequency dependence of their dielectric parameters. Correct simulations should be based on the experimentally measured spectra of the complex dielectric permittivity. The last approach was successfully applied (see [11,12] for instance), even if the dielectric spectra were measured in the relatively narrow frequency range. We propose combination of the experimental and simulation approaches and present analysis of shielding and absorption efficiency of composites based on the experimentally measured broadband dielectric spectra, including HF, MW and THz ranges.

3.1. Calculations of Shielding and Absorbing Efficiency

To estimate the shielding and absorption properties, we relate them to the dielectric spectra of composites by analysis of EM wave interaction with the composite layer (absorber) in free space. Two model configurations were analyzed: a) EM wave transmission through a single layer; b) EM wave reflection from the layer backed by a perfect electric conductor. The EM wave was considered to be normally incident. The characteristic impedance Z_2 and propagation constant γ of the absorber are defined by the complex dielectric permittivity and magnetic permeability (μ^*) of a composite [7,9,10]:

$$Z_2 = Z_0\sqrt{\frac{\mu^*}{\varepsilon^*}},\ \gamma = \frac{i\omega\sqrt{\mu^*\varepsilon^*}}{c}, \tag{1}$$

where Z_0 = 377 Ohm is the characteristic impedance of the free space and c is the speed of light in free space. The characteristic impedances Z_1 and Z_3 of the semi-infinite media are equal to Z_0 in the case of free space or air. Considering the metal plate as a perfect electric conductor, we suppose its impedance $Z_3 = 0$ [9]. Then the input wave impedance Z_{in} of the analyzed structures at the surface of the absorber can be defined, according to the transmission line theory [7,10], as

$$Z_{in} = Z_2\frac{Z_3\cosh(\gamma d) + Z_2\sinh(\gamma d)}{Z_2\cosh(\gamma d) + Z_3\sinh(\gamma d)}, \tag{2}$$

where d is the layer thickness. In the model of EM wave transmission, Eq. 2 can be transformed to

$$Z_{in} = \sqrt{\frac{\mu^*}{\varepsilon^*}}Z_0\frac{1+\sqrt{\frac{\mu^*}{\varepsilon^*}}\tanh(\gamma d)}{\sqrt{\frac{\mu^*}{\varepsilon^*}}+\tanh(\gamma d)} \tag{3}$$

Then transmission coefficient (T) can be defined [6,7,10] as following:

$$\tau = \frac{2Z_{in}}{Z_{in}+Z_1},\ T = 20\log|\tau| \tag{4}$$

The shielding efficiency SE is estimated as $SE = -T$.

Excerpt from ISBN 978-3-00-053387-7

In the second model of EM wave reflection, Eq. 2 can be transformed to

$$Z_{in} = \sqrt{\frac{\mu^*}{\varepsilon^*}} Z_0 \tanh(\gamma d)\,. \tag{5}$$

Then frequency dependences of the reflection loss (*RL*) and attenuation constant α (real part of the propagation constant γ) of the material, in neper/m, can be calculated as following [7,9]:

$$RL = 20\log|\rho| = 20\log\left|\frac{\sqrt{\frac{\mu^*}{\varepsilon^*}}\tanh(\gamma d) - 1}{\sqrt{\frac{\mu^*}{\varepsilon^*}}\tanh(\gamma d) + 1}\right|, \tag{6}$$

$$\alpha = \mathrm{Re}(\gamma) = \mathrm{Re}\left(\frac{i\omega\sqrt{\mu^*\varepsilon^*}}{c}\right), \tag{7}$$

Reflection loss and attenuation constant characterize the MW absorption efficiency *MA*, which could be numerically estimated as $MA = -RL$.

3.2. Shielding efficiency and microwave absorption of PET-xCNT and PANI

We used experimental dielectric spectra of PET-CNT composites or their fits shown in Fig. 1 to estimate the shielding efficiency *SE* and microwave absorption *MA* in the MW and THz ranges. The magnetic field effects were neglected in the quasi-static approximation and the value $\mu^* = 1 - i0$ was used in Equations (1-7). *SE* and *MA* were calculated in dependence on the CNT concentration, layer thickness (d = 0.1 – 10 mm) and frequency. Selected results are shown in Figures 5 and 6.

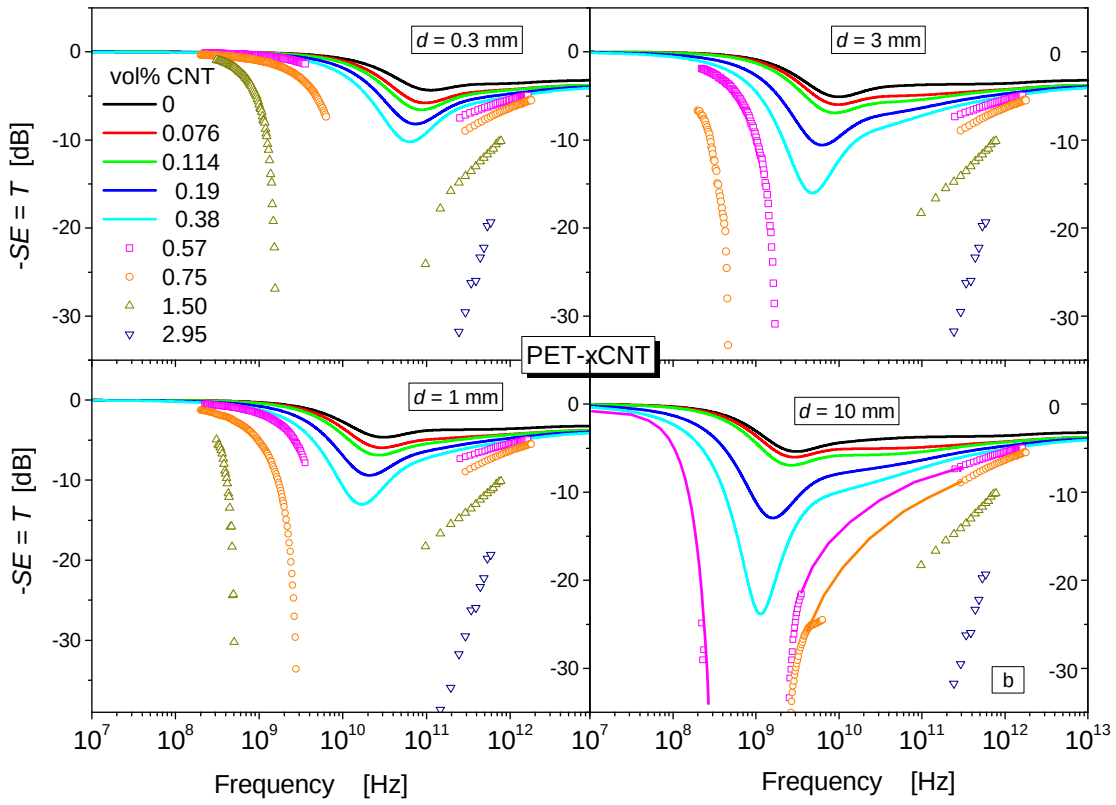

Figure 5. Shielding efficiency *SE* of PET-xCNT composites.

Excerpt from ISBN 978-3-00-053387-7

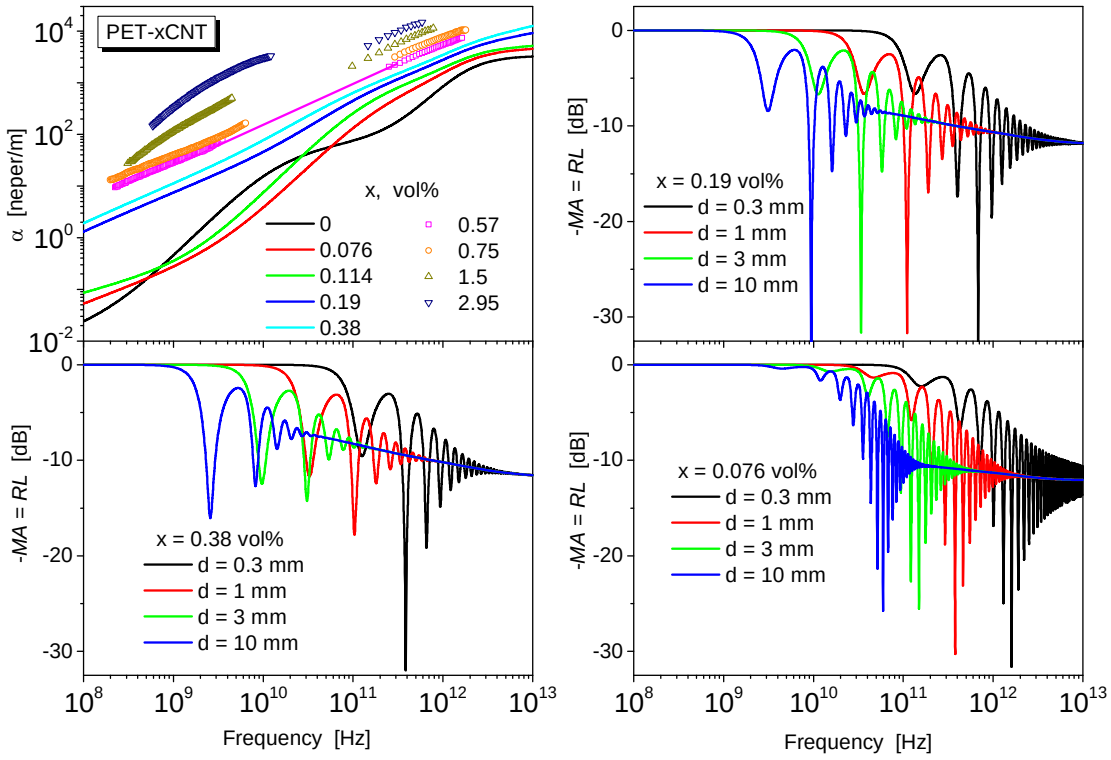

Figure 6. Microwave absorption *MA* of PET-xCNT composites.

SE values up to 35 dB can be achieved at frequencies from 0.3 GHz to 500 GHz, depending on the CNT concentration x and layer thickness *d*. Increase of x and *d* results in the increase of *SE* and in the shift down of the high-*SE* frequency band corresponding to the broad minimum of *T*-coefficient (Fig. 5). The frequency band of high-*SE* is broad and achieves a decade of frequency at the 30 dB level, which is very important for the shielding applications. For composites with high CNT concentration, x > 0.75 vol.%, MW absorption is not effective. For the lower CNT concentration, *MA* values up to 30 dB can be achieved at frequencies from 2 to 1000 GHz, depending on the CNT concentration and layer thickness. Increase of x and *d* results in the increase of *MA* and in the shift down of the high-*MA* frequency band (Fig. 6). The frequency bands of high-*MA* are narrow and multiple, different from the high-*SE* band, which is single and broad. The attenuation constant α reaches 100 neper/m in the GHz and 1000 neper/m in the THz ranges. Increase of x results in the increase of α. High values of the attenuation constant are important for the absorbing applications of PET-CNT composites.

Phenomenological fits of PANI dielectric spectra [2] were used for calculations of shielding and absorption efficiency calculations of the nc-PANI, sc-PANI and c-PANI layers in dependence on the layer thickness (d = 0.1 – 10 mm) and frequency. Shielding efficiency of the nc-PANI and sc-PANI layers does not exceed 10 dB, while *SE* of the c-PANI layers can achieve 40 dB in a broad frequency band in the MW range. The 0.3 mm thin c-PANI layer provides the 20 dB *SE* band between 10 MHz and 50 GHz. Such a high level of shielding efficiency of the conductive PANI is mainly caused by the DC conductivity contribution. MW absorption of the c-PANI layers is not effective. For the nc-PANI and sc-PANI layers, *MA* values up to 20 dB can be achieved at frequencies from 10 GHz to 1 THz, depending on the layer thickness. The frequency bands of high-*MA* are narrow and multiple in the case of nc-PANI and sc-PANI, different from the single and broad high-*SE* band of the c-PANI layers. The attenuation constant α can be varied from 0.1 neper/m to 10 000 neper/m in the range of 0.1÷100 GHz depending on the level of PANI DC conductivity. High values of the attenuation constant are important for the absorbing applications of PANI.

Excerpt from ISBN 978-3-00-053387-7

3. Conclusions

Broadband dielectric spectroscopy (1 mHz – 1 THz) was shown to be an effective tool for study and development of DCC. BDS can reveal essential information on the composition-structure-properties relation, conductivity mechanisms on various length scales down to sub-nm, percolation phenomena, etc. of dielectric-conductor composites. BDS can be also effectively used for analysis of the shielding efficiency and microwave absorption of DCC in the high-frequency, microwave and THz ranges that allows estimation of their potential for the electromagnetic applications. DCC were shown to be promising MW and THz shielding and absorbing materials. Their properties can be effectively controlled by changing the concentration of conductive fillers. PET-xCNT composites are interesting for both shielding and absorbing applications. For the absorbing applications, low-x compositions ($0 < x < 0.75$ vol.%) can be used; for the shielding ones, high-x compositions ($x > 0.2$ vol.%) are preferable. Variously conductive PANI show a high level of the shielding efficiency (c-PANI) or microwave absorption (sc-PANI and nc-PANI), depending on their DC conductivity level.

Acknowledgments

This work was supported by the Czech Science Foundation (Project No. 15-08389S).

References

[1] J.C. Dyre and T.B. Schroder. Universality of ac conduction in disordered solids. *Rev. Mod. Phys*. **72**, 873-892, 2000.

[2] J. Petzelt, D. Nuzhnyy, V. Bovtun, M. Savinov, M. Kempa, I. Rychetsky. Broadband dielectric and conductivity spectroscopy of inhomogeneous and composite conductors. *Phys. Status Solidi A*, **210** (11), 2259–2271, 2013.

[3] D. Nuzhnyy, M. Savinov, V. Bovtun, M. Kempa, J. Petzelt, et al. Broad-band conductivity and dielectric spectroscopy of composites of multiwalled carbon nanotubes and poly(ethylene terephthalate) around their low percolation threshold. *Nanotechnology* **24**, 055707, 1-9, 2013.

[4] L. Fernandez-Garcia, M. Suarez, J.L. Menendez, C. Pecharroman, D. Nuzhnyy, V. Bovtun, et al. Dielectric properties of carbon nanofibre/alumina composites. *Carbon* **57**, 380-387, 2013.

[5] P. Sheng. Fluctuation-induced tunneling conduction in disordered materials. *Phys. Rev. B* **21**, 2180-2195, 1980.

[6] H.W. Ott, *Electromagnetic Compatibility Engineering*, I. Wiley & Sons, New York, 2009.

[7] J. Vinoy and R.M. Jha, *Radar Absorbing Materials - from Theory to Design and Characterization*, Kluwer Academic Publishers, Boston, MA, 1996.

[8] *Polymer-Carbon Nanotube Composites: Preparation, Properties and Applications*, Ed. T. McNally and P. Pötschke, Woodhead Publ., Oxford, 2011.

[9] F. Qin and C. Brosseau. A review and analysis of microwave absorption in polymer composites filled with carbonaceous particles. *J. Appl. Phys.* **111**, 061301, 1-24, 2012.

[10] F. Nani, M. Valentini. Electromagnetic properties of polymer-carbon nanotube composites. – In *Polymer-Carbon Nanotube Composites: Preparation, Properties and Applications*, Ed. T. McNally and P. Pötschke, Woodhead Publ., Oxford, 2011, pp. 329-346.

[11] C.Y. Tsay, R.B. Yang, D.S. Hung, Y.H. Hung, Y.D.Yao, and C.K. Lin. Investigation on electromagnetic and microwave absorbing properties of $La_{0.7}Sr_{0.3}MnO_{3-\delta}$/carbon nanotube composites, *J. Appl. Phys*. **107**, 09A502, 1-3, 2010.

[12] R.K. Srivastava, T.N. Narayanan, A.P. R. Mary, M.R. Anantharaman, A. Srivastava, R. Vajtai, and P.M. Ajayan. Ni filled flexible multi-walled carbon nanotube–polystyrene composite films as efficient microwave absorbers, *Appl. Phys. Lett.* **99**, 113116, 1-3, 2011.

Excerpt from ISBN 978-3-00-053387-7